

Liquid Crystalline Properties of Polyguanidines

Jeonghan Kim and Bruce M. Novak*

Department of Chemistry, North Carolina State University, Raleigh, North Carolina 27695

Alan John Waddon

Department of Polymer Science & Engineering, University of Massachusetts, Amherst, Massachusetts 01003

Received April 1, 2004; Revised Manuscript Received August 13, 2004

ABSTRACT: Modified polyguanidines were prepared, and their liquid crystalline properties were studied using optical polarizing microscopy and X-ray diffraction. Parameters examined include chirality, the uniformity of the lengths of side chains, and attached side-chain mesogens. If the side chains on the repeat units are identical, then polymer has a more ordered structure in both solution and the solid state. Uniform lengths of the side chains are also important. Poly(*N,N*-di-*n*-hexylguanidine), poly-**I**, exhibited a lyotropic smectic texture in contrast to a nematic texture of poly(*N*-(*rac*-2-phenylethyl)-*N*-methylguanidine) (poly-**(rac-II)**). Optically pure poly(*N*-((*R*)-2-phenylethyl)-*N*-methylguanidine) (poly-**(R-II)**) formed a cholesteric texture, whereas the corresponding racemic polyguanidine, poly-**(rac-II)**, formed a nematic texture. Additionally, poly-**(R-II)** displayed a mesophase at a lower critical concentration than either poly-**I** or poly-**(rac-II)**, implying that poly-**(R-II)** is stiffer than these two other derivatives. Poly(*N*-6-((4'-methoxyphenylazo)phenyl-4-oxy)hexyl-*N*-*n*-hexylguanidine) (poly-**IV**), one of combined liquid crystalline structures (liquid crystalline backbone plus liquid crystalline side chains), displayed a lyotropic nematic texture presumably due to the strong dipolar–dipolar interaction between the main chain and side chains that folds the appendages parallel to the molecular axis. Poly(*N*-12-((4'-methoxybiphenyl-4-oxy)dodecyl-*N*-*n*-dodecylguanidine) (poly-**V**) and poly(*N,N*-di-*n*-dodecylguanidine) (poly-**VI**) exhibited thermotropic liquid crystalline behavior.

Introduction

Because of their stiffness, many helical polymers show lyotropic main-chain liquid crystalline properties since the helix behaves as a mesogen. Lyotropic mesophases of polypeptides,^{1–10} polyisocyanides,^{11–14} and polyisocyanates^{15–22} have been identified and reported. During our efforts to develop new helical materials, we found that carbodiimides can be polymerized in a living fashion using a variety of transition metal complexes.^{23,24} The polycarbodiimides (or polyguanidines) are rigid chain helical polymers with high inversion barriers and long persistence lengths. In keeping with these intramolecular characteristics, we found that these polymers display a range of liquid crystalline phases. We recently reported on the lyotropic smectic liquid crystalline properties of poly(*N,N*-di-*n*-hexylguanidine), poly-**I**.²⁵ Poly-**I** displays a lyotropic layered structure a over broad concentration range ($\geq 16\%$ (w/w)) in toluene at ~ 45 °C.²⁶ The smectic layering arises from the dense, uniform corona formed by the hexyl side chains, which allows the chains to align in a uniform fashion.²⁵ In this study, polyguanidines with various stereochemical and molecular architectural modifications were prepared, and their lyotropic liquid crystalline properties were examined. Most polyguanidines are limited to lyotropic studies because these polymers selectively decompose back to their monomers at temperatures below any melt transitions. Herein, we report two thermotropic exceptions to this generalization.

Experiment

General. All glassware was either flame-dried or oven-dried overnight. Unless otherwise noted, all solvents were reagent grade and used without further purification except for drying either over 3 Å molecular sieves or by inert atmosphere

chromatography. Polymerizations were conducted in an inert atmosphere drybox or on vacuum lines.

Synthesis of Monomers. *N*-Methyl-*N*-((*R*)-(+)-(α)-methylbenzylthiourea. The same procedure for the preparation of *N,N*-di-*n*-hexylurea was employed as reported previously.²⁷

***N*-Methyl-*N*-((*R*)-(+)-(α)-methylbenzyl)carbodiimide, **R-II.** A dry 1 L round-bottom flask was charged with 500 mL of acetone, 10.0 g of *N*-methyl-*N*-((*R*)-(+)-(α)-methylbenzyl)thiourea (51.5 mmol), and a magnetic stir bar. The resulting solution was heated to reflux. 44.6 g of mercury oxide (0.206 mol, 4 equiv) was added in five equivalent portions to the hot *N*-methyl-*N*-((*R*)-(+)-(α)-methylbenzylthiourea solution over 1 h, and the resulting solution was heated at refluxed for an additional hour. The solution turned to dark green, and a solution was filtered through a glass filter. The acetone was distilled off to give light yellow oil. The oil was washed with 500 mL of *n*-hexane, and the residue was removed under vacuum. The resulting oil was distilled under reduced pressure to give *N*-methyl-*N*-((*R*)-(+)-(α)-methylbenzyl)carbodiimide as a clear, colorless liquid. Yield: 4.90 g (51%); bp = 55 °C (0.1 Torr). ¹H NMR (300 MHz, CDCl₃): δ (ppm) 1.48 (d, 3H, CH₃), 2.89 (s, 3H, CH₃), 4.62 (q, 1H, CH), 7.3 (m, 5H, Ar). IR (neat): 3055 (m), 2908 (s), 2935 (s), 2124 (vs), 1492 (s), 1452 (s), 1421 (s), 1372 cm⁻¹ (s). ¹³C NMR (CDCl₃): 173.72, 152.37, 132.11, 131.89, 131.47, 130.90, 130.27, 129.98, 37.34, 28.73. Anal. Calcd for C₁₀H₁₂N₂: C, 74.95; H, 7.55; N, 17.50. Found: C, 75.21; H, 7.43; N, 17.36.**

***N,N*-Di-*n*-dodecylurea.** A 250 mL round-bottom flask was charged with 8.40 g of *n*-dodecylamine (0.110 mol), a magnetic stir bar, and 150 mL of reagent grade dry toluene. The resulting solution was cooled to 0 °C by the use of an ice bath. A dry pressure equalizing additional funnel was charged with 50 mL of toluene and 8.40 g of 1,1'-carbonyldiimidazole (51.8 mmol) and was then placed on the 250 mL round flask. The whole apparatus was placed under a nitrogen atmosphere. The 1,1'-carbonyldiimidazole solution was added dropwise over the course of 30 min, and the resulting solution was refluxed for 3 h. The solution was cooled to room temperature. The white solid *N,N*-di-*n*-dodecylurea was obtained by removing the

toluene using rotary evaporator and recrystallized in ethanol. Yield: 20.3 g (95%). This product was carried forward without further purification.

***N,N*-Di-*n*-dodecylcarbodiimide, VI.** A dry 500 mL round-bottom flask was charged with 300 mL of dichloromethane, 15.7 g of triphenylphosphine (59.9 mmol, 25% excess), and a magnetic stir bar. A dry pressure equalizing addition funnel was charged with 30 mL of dichloromethane and 3.09 mL of bromine (59.9 mmol, 25% excess) and was then placed on the 500 mL round-bottom flask. The whole apparatus was placed under a nitrogen atmosphere, and the triphenylphosphine solution was cooled to 0 °C. The bromine solution was added dropwise over the course of 30 min, and the resulting solution was allowed to stir for an additional 10 min. To the resulting suspension of dibromotriphenylphosphorane, 16.7 mL of triethylamine (0.120 mol, 26% excess) was added. In a similar fashion, 18.5 g of *N,N*-di-*n*-dodecylurea (47.8 mmol) was added in five equivalent portions to the 0 °C suspension over the next hour. One hour after the last addition of the urea, 100 mL of water was poured to the round-bottom flask in order to extract the triethylammonium hydrobromide, and organic and aqueous phases were separated using a separatory funnel. The dichloromethane was distilled off using a rotary evaporator. Addition of 300 mL of *n*-hexane to the viscous, dark brown oil served to remove the triphenylphosphine oxide. The *n*-hexane was distilled off to give light yellow oil. The remaining triphenylphosphine oxide was removed in acetonitrile. *N,N*-Di-*n*-dodecylcarbodiimide was obtained through vacuum distillation. Yield: 13.8 g (76%); bp = 122 °C (0.1 Torr). ¹H NMR (300 MHz, CDCl₃): δ (ppm) 0.90 (t, 6H, CH₃), 1.35 (m, 36H, CH₂), 1.55 (m, 4H, CH₂), 3.11 (t, 4H, CH₂). ¹³C NMR (CDCl₃): 171.89, 53.26, 36.88, 36.73, 36.05, 35.96, 35.78, 35.67, 34.99, 34.04, 32.89, 32.54, 31.81. IR (neat): 2923 (vs), 2852 (vs), 2129.6 (vs), 1466.7 (m), 1440.3 cm⁻¹ (m). Anal. Calcd for C₂₅H₅₀N₂: C, 79.29; H, 13.31; N, 7.40. Found: C, 79.02; H, 13.44; N, 7.54.

***N*-Methyl-*N*-((±)-(α-methylbenzyl)thiourea.** The same procedure for the preparation of *N*-methyl-*N*-((*R*)-(+)-(α-methylbenzyl)thiourea was employed.

***N*-Methyl-*N*-((±)-(α-methylbenzyl)carbodiimide, rac-II.** The same procedure for the preparation of *N*-methyl-*N*-((*R*)-(+)-(α-methylbenzyl)carbodiimide was employed.

7-Bromoheptanoyl Chloride. To a 500 mL Schlenk flask was added 125 g of 7-bromoheptanoic acid (0.600 mol, 1 equiv)²⁸ and 142 g of thionyl chloride (0.231 L, 1.19 mol, 2 equiv). The mixture was heated to 50 °C and then stirred for 4 h. The excess thionyl chloride was removed using a rotary evaporator to give yellow liquid. 7-bromoheptanoyl chloride was obtained under reduced pressure. Yield: 121 g (89%); bp = 60 °C (0.1 Torr). ¹H NMR (300 MHz, CDCl₃): δ (ppm) 1.3–1.5 (m, 4H, CH₂), 1.70–1.80 (m, 2H, CH₂), 1.80–1.90 (m, 2H, CH₂), 2.9 (t, 2H, CH₂), 3.40 (t, 2H, CH₂). IR (neat): 2938 (s), 2861 (s), 1799 (vs), 1459 (w), 1406 (w), 953 (w) cm⁻¹.

6-Bromoheptyl Isocyanate. To a 500 mL Schlenk flask equipped with a condenser and nitrogen inlet was added 121 g of 7-bromoheptanoyl chloride (0.530 mol, 1 equiv) followed by 100 mL of toluene. 69.5 g of azidotrimethylsilane (42.6 mL, 0.580 mol, 1.1 equiv) was added to the mixture and stirred at room temperature for 30 min. The temperature was increased to 50 °C for 30 min and then refluxed for 20 h. The yellow liquid was distilled under reduced pressure to give colorless liquid. Yield: 60.1 g (55%); bp = 60 °C (0.15 Torr). ¹H NMR (300 MHz, CDCl₃): (ppm) 1.4–1.19 (m, 8H, CH₂), 3.3 (t, 2H, CH₂), 3.45 (t, 2H, CH₂). ¹³C NMR (CDCl₃): 133.35, 51.13, 45.36, 37.78, 33.38, 32.23, 31.99. IR (neat): 2928 (s), 2869 (m), 2257 cm⁻¹ (vs). Anal. Calcd for C₂₆H₃₆N₂O₂: C, 40.80; H, 5.87; Br, 38.77; N, 6.80; O, 7.76. Found: C, 41.19; H, 5.85; Br, 38.42; N, 6.55; O, 7.99.

***N*-6-Bromoheptyl-*N*-hexylurea.** A 250 mL round-bottom flask was charged with 8.60 g of 6-bromoheptyl isocyanate (41.7 mmol), a magnetic stir bar, and 50 mL of reagent grade dry chloroform. The resulting solution was cooled to 0 °C by the use of an ice bath. Over the next 30 min, 5.50 mL of *n*-hexylamine (4.20 g, 41.3 mmol, 0.99 equiv) was added dropwise to the cooled solution. An additional 20 mL of

chloroform was used to ensure complete transfer of *n*-hexylamine. The resultant solution was stirred for 1 h. The white solid, *N*-6-bromoheptyl-*N*-hexylurea, was obtained by removing the chloroform using rotary evaporator and then recrystallized in ethanol. Yield: 12.3 g (97%). ¹H NMR (300 MHz, CDCl₃): (ppm) 0.89 (t, 3H, CH₃), 1.2–1.6 (m, 14H, CH₂), 1.85 (t, 2H, CH₂), 3.15 (m, 4H, CH₂), 3.40 (t, 2H, CH₂), 4.22 (s, br, 2H, NH). IR (KBr pellet): 3420 (s, br), 2955 (w), 2930 (m), 2869 (m), 1660 (s), 1630 cm⁻¹ (s).

***N*-6-(4'-Methoxybiphenyl-4-oxy)hexyl-*N*-*n*-hexylurea.** To a 1 L round-bottom flask was added 2.50 g of *N*-6-bromoheptyl-*N*-hexylurea (8.14 mmol, 1 equiv) and 100 mL of ethanol as a solvent. The whole apparatus was placed under a nitrogen atmosphere. To a 250 mL round-bottom flask was added 1.63 g of 4'-methoxybiphenyl-4-ol (8.14 mmol, 1 equiv),²⁹ 0.460 g of potassium hydroxide (8.20 mmol, 0.99 equiv), 40 mL of ethanol, and 10 mL of water. The 4'-methoxybiphenyl-4-ol solution was added to the *N*-6-bromoheptyl-*N*-hexylurea solution. The resulting solution was heated to reflux overnight. The solution was filtered to give white powder. The white powder was washed with fresh white ethanol. Yield: 1.63 g (50%). ¹H NMR (300 MHz, CDCl₃): δ (ppm) 0.89 (t, 3H, CH₃), 1.2–1.6 (m, 14H, CH₂), 1.85 (t, 2H, CH₂), 3.20 (m, 4H, CH₂), 3.85 (s, 3H, CH₃), 4.01 (t, 2H, CH₂), 4.18 (d, br, 2H, NH), 6.95 (m, 4H, Ar), 7.50 (m, 4H, Ar). IR (NaCl pellet): 3320 (s, br), 3300 (s, br), 3050 (w), 2955 (w), 2930 (m), 2869 (m), 1660 (s), 1630 cm⁻¹ (s).

***N*-6-(4'-Methoxybiphenyl-4-oxy)hexyl-*N*-*n*-hexylcarbodiimide, III.** The same procedure for the preparation of *N,N*-di-*n*-hexylcarbodiimide was employed.²⁷ The quantities of reagents used were 1.92 g of *N*-6-(4'-methoxybiphenyl-4-oxy)hexyl-*N*-*n*-hexylurea (4.50 mmol, 1 equiv), 1.48 g of triphenylphosphine (5.64 mmol, 1.25 equiv), 0.290 mL of bromine (0.900 g, 5.64 mmol, 1.25 equiv), 1.97 mL of triethylamine (1.43 g, 11.3 mmol, 2.5 equiv), and 55 mL of dichloromethane. The crude product from evaporation of *n*-pentane is recrystallized in warm acetonitrile to give white powder. Yield: 1.1 g (60%). ¹H NMR (300 MHz, CDCl₃): δ (ppm) 0.89 (t, 3H, CH₃), 1.2–1.6 (m, 14H, CH₂), 1.85 (t, 2H, CH₂), 3.25 (m, 4H, CH₂), 3.85 (s, 3H, CH₃), 4.01 (t, 2H, CH₂), 6.95 (m, 4H, Ar), 7.40 (m, 4H, Ar). ¹³C NMR (CDCl₃): δ (ppm) 173.99, 168.24, 163.35, 133.43, 133.26, 133.03, 132.94, 132.56, 131.23, 121.68, 121.23, 121.02, 120.85, 87.69, 60.70, 57.64, 57.55, 37.84, 37.24, 37.18, 37.01, 31.80, 31.52, 30.90, 30.24, 18.32. IR (neat): 3067 (w), 3037 (w), 2932 (vs), 2865 (vs), 2151 (vs), 2127 (vs), 1608 (w), 1503 (s), 1467 (m), 1338 (m), 1276 (s), 1252 cm⁻¹ (s). Anal. Calcd for C₂₆H₃₆N₂O₂: C, 76.43; H, 8.88; N, 6.86. Found: C, 76.22; H, 8.87; N, 6.67.

4-(4-Methoxyphenylazo)phenol. To a 100 mL round-bottom flask was added 10.0 g of *p*-anisidine (81.2 mmol, 1 equiv) and 20.0 mL of water. 6.70 mL of 37% hydrochloric acid (81.2 mmol, 1 equiv) was added to the *p*-anisidine solution. The solution was cooled below 10 °C. To a 100 mL beaker was added 5.60 g of sodium nitrite (81.2 mmol, 1 equiv) and 50.0 mL of water. The sodium nitrite solution was cooled below 10 °C. The sodium nitrite solution was added dropwise to the cooled *p*-anisidine solution. After allowing the solution to stir for 2 h at 10 °C, the solution was added dropwise to the solution of 7.64 g of phenol, 3.25 g of sodium hydroxide, 9.00 g of sodium carbonate, and 100 mL of water at 10 °C. 1 h after the last addition of diazonium salt solution, the solution was neutralized using 37% of hydrochloric acid. The suspended solid was filtered to give dark brown solid. The crude product was recrystallized in mixed solvent of methanol and water (50%) to give the brown solid. Yield: 14.76 g (80%); mp = 149.8 °C. ¹H NMR (300 MHz, CDCl₃): δ (ppm) 3.95 (s, 3H, CH₃), 6.84 (d, 2H, Ar), 6.92 (d, 2H, Ar), 7.75–7.79 (m, 4H, Ar). ¹³C NMR (CDCl₃): δ (ppm) 170.24, 167.31, 152.43, 151.78, 133.98, 132.74, 130.29, 128.33, 120.66, 120.01, 119.19, 118.72, 60.80.

***N*-6-(4-(4-Methoxyphenylazo)phenyloxy)hexyl-*N*-*n*-hexylurea.** The same procedure for the preparation of *N*-6-(4'-methoxybiphenyl-4-oxy)-hexyl-*N*-*n*-hexylurea was employed. The quantities of reagents used were 10.0 g of 4-(4-methoxyphenylazo)phenol (44.0 mmol, 1 equiv), 13.5 g of *N*-6-bromoheptyl-*N*-hexylurea (44.0 mmol, 1 equiv), 2.47 g of

potassium hydroxide (44.0 mmol, 1 equiv), 500 mL of ethanol, and 10.0 mL of water. Yellow solid. Yield: 11.20 g (57%). This product was used for the next reaction without further purification.

N-6-(4-(4-Methoxyphenylazo)phenyloxy)hexyl-*N*-*n*-hexylcarbodiimide, IV. The same procedure for the preparation of *N,N*-dibenzylurea was employed. The quantities of reagents used were 5.00 g of *N*-6-(4-(4-methoxyphenylazo)phenyloxy)hexyl-*N*-*n*-hexylurea (11.2 mol, 1 equiv), 3.67 g of triphenylphosphine (14.0 mmol, 1.25 equiv), 0.720 mL of bromine (2.24 g, 5.64 mmol, 1.25 equiv), 3.90 mL of triethylamine (2.83 g, 28.0 mmol, 2.5 equiv), and 110 mL of dichloromethane. The crude product from evaporation of *n*-pentane was recrystallized in diethyl ether to give yellow powder. Yield: 3.5 g (70%); mp = 63.1 °C. ¹H NMR (400 MHz, CDCl₃): δ (ppm) 0.89 (t, 3H, CH₃), 1.20–1.65 (m, 14H, CH₂), 1.85 (m, 2H, CH₂), 3.25 (m, 4H, CH₂), 3.85 (s, 3H, CH₃), 4.05 (t, 2H, CH₂), 6.95 (m, 4H, Ar), 7.40 (m, 4H, Ar). IR (neat): 3099 (w), 3057 (w), 2938 (s), 2861 (s), 2151 (vs), 2133 (vs), 1603 (m), 1579 (m), 15–1 (m), 1465 (m), 1251 (s), 1149 (s), 1030 (m), 845 cm⁻¹ (s). Anal. Calcd for C₂₆H₃₆N₄O₂: C, 71.53; H, 8.31; N, 12.86. Found: C, 71.71; H, 8.46; N, 13.00.

13-Bromotridecanoic Acid.³⁰ To a 1 L round-bottom flask was added 378 mL of ethanol. 17.5 g (0.760 mol) of chopped sodium metal was slowly added to the flask (sodium metal was washed with *n*-hexane before use). 243 g of diethylmalonate (1.52 mol, 2 equiv) was added to the sodium ethoxide solution. The resulting solution was added dropwise to the solution of 96.0 g of 11-bromo-1-undecanol (0.380 mol, 0.5 equiv) in 100 mL of ethanol at 25 °C. The resulting solution was heated to reflux for 5 h. The resultant solution was poured into 1 L of ice water and extracted with diethyl ether. The extract was dried over sodium sulfate, and the diethyl ether was distilled off using a rotary evaporator. The solution of 102 g of potassium hydroxide in 300 mL of water was added to the residue and then heated reflux for 4 h. The resultant solution was poured into 200 mL of ice water, acidified with concentrated hydrochloric acid, and then extracted with diethyl ether. The diethyl ether was distilled off using a rotary evaporator. 800 mL of hydrobromic acid in glacial acetic acid was added to the residue. The resulting solution was allowed to stir at room temperature for 15 h and then heated to 100 °C for 8 h. The solvent was distilled off, and then the residue was heated to 160 °C until CO₂ was completely escaped. A dry 1 L round-bottom flask was charged with the liquid, 500 mL of glacial acetic acid, 100 mL of sulfuric acid, and a magnetic stir bar. The resulting solution was refluxed for 1 day, with a warm condenser allowing ethyl acetate to escape. The residue was cooled to room temperature to give the crude solid product. It was recrystallized in petroleum ether to give white solid. Yield: 90.7 g (81%); mp = 53 °C. ¹H NMR (400 MHz, CDCl₃): δ (ppm) 1.3–1.9 (m, 20H, CH₂), 2.30 (t, 2H, CH₂), 3.33 (t, 2H, CH₂). ¹³C NMR (400 MHz, CDCl₃): δ (ppm) 167.22, 36.24, 33.67, 32.13, 30.15, 30.12, 30.10, 30.08, 30.01, 29.80, 29.26, 28.67, 27.33.

N-12-(4'-Methoxybiphenyl-4-oxy)dodecyl-*N*-*n*-dodecylcarbodiimide, V. The same procedure for the preparation of *N*-6-(4'-methoxybiphenyl-4-oxy)-hexyl-*N*-*n*-hexylcarbodiimide was employed. The quantities of reagents used were 3.00 g of *N*-12-(4'-methoxybiphenyl-4-oxy)dodecyl-*N*-*n*-dodecylurea (5.78 mmol, 1 equiv), 3.79 g of triphenylphosphine (14.4 mmol, 2.5 equiv), 1.46 g of triethylamine (14.4 mmol, 2.5 equiv), and 2.30 g of Br₂. Yield: 1.42 g (49%). ¹H NMR (300 MHz, CDCl₃): δ (ppm) 0.89 (t, 3H, CH₃), 1.2–1.6 (m, 40H, CH₂), 1.85 (t, 2H, CH₂), 3.25 (m, 4H, CH₂), 3.85 (s, 3H, CH₃), 4.01 (t, 2H, CH₂), 6.95 (m, 4H, Ar), 7.40 (m, 4H, Ar). ¹³C NMR (CDCl₃): δ (ppm) 173.56, 167.35, 164.21, 132.78, 132.33, 132.21, 132.02, 131.88, 131.57, 122.79, 122.12, 121.90, 120.79, 90.24, 61.34, 58.13, 57.83, 37.84, 37.24, 37.18, 37.01, 32.43, 32.21, 32.04, 31.80, 31.52, 31.22, 31.02, 30.90, 30.78, 30.53, 30.39, 30.24, 30.11, 29.85, 29.58, 29.27, 18.32. IR (neat): 3067 (w), 3037 (w), 2932 (vs), 2865 (vs), 2151 (vs), 2127 (vs), 1608 (w), 1503 (s), 1467 (m), 1338 (m), 1276 (s), 1252 cm⁻¹ (s). Anal. Calcd for C₃₈H₆₀N₂O₂: C, 79.17; H, 10.42; N, 4.17. Found: C, 78.73; H, 10.21; N, 4.10.

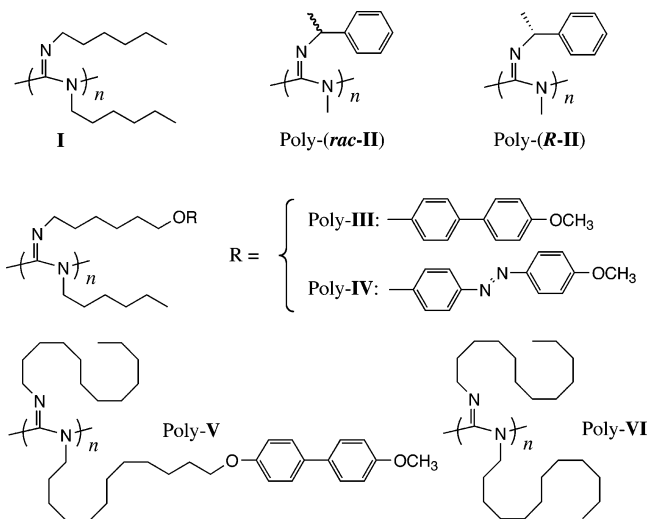
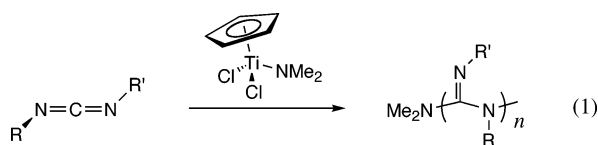


Figure 1. Structures of the liquid crystalline polyguanidines used in this study.

General Method for the Polymerization of Carbodiimides. The following description serves as a general method for the polymerization of carbodiimides having mesogenic side chains. Prior to sealing ampules, all manipulations were performed in a glovebox. The highest concentrated solution of *N*-6-(4'-methoxybiphenyl-4-oxy)hexyl-*N*-*n*-hexylcarbodiimide was prepared in chloroform because the yield and the conversion depend on the concentration of monomer solution (1.46 g of the monomer dissolved in 8.74 g of chloroform (molar concentration is 0.609 mol/L)). The prepared solution was added via syringe to an ampule (10 mL) containing a stirbar. (Note: these ampules were made from Pasteur pipets (146 mm). The wide end of the pipet was cut just below the indentation, and a stirbar was inserted into the pipet. The wide end was then sealed with a glass blower's torch.) 0.176 g of the titanium catalyst (0.776 mmol) was added to a volumetric flask (5 mL) and dissolved in 1 mL of chloroform. 0.100 mL of the catalyst solution was added to the ampule via syringe and quickly stirred to ensure proper mixing. The ampule was then plugged with grease, removed from the glovebox, and cooled in liquid nitrogen. After the contents froze, the ampule was sealed with a glass blower's torch and allowed to warm to room temperature. The samples were then stirred until gelation. After the samples have gelled, methanol was added to the ampules. The color of the solution disappeared, and then white powder was precipitated. The precipitated polymer was filtered and then dissolved in chloroform. The polymer was precipitated into stirring methanol. After the precipitation is complete, the polymer is filtered through a Büchner funnel and dried under reduced pressure. In IR, the characteristic peak of carbodiimide monomer (stretching of -N=C=N-) was observed. The unreacted monomer was completely extracted out in *n*-hexane, using Soxhlet extraction.

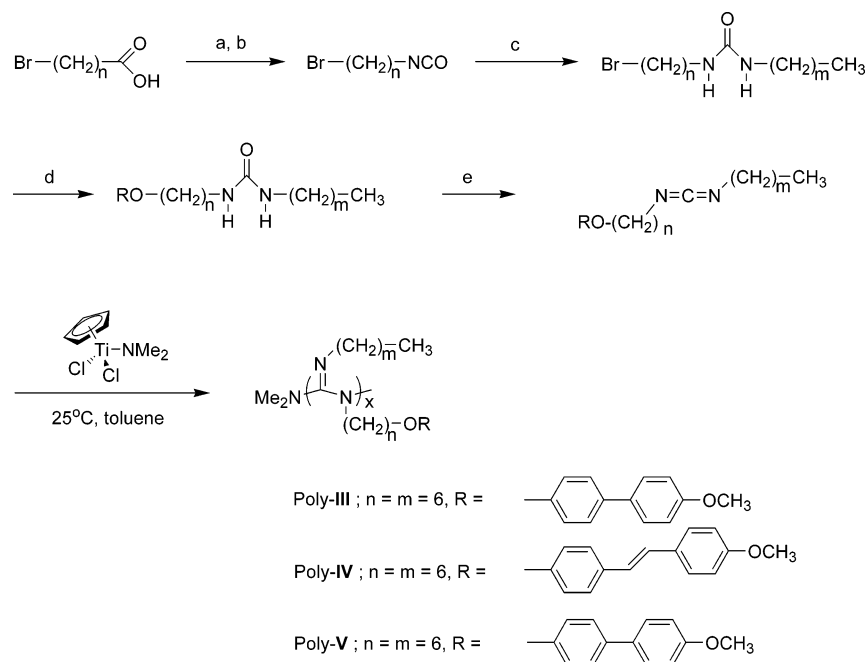
Results and Discussion

All of the polyguanidines used in this study were prepared by polymerizing the corresponding carbodiimide monomers using dichloro(η^5 -cyclopentadienyl)-(dimethylamido)titanium as a catalyst (eq 1).²³



The chemical structures of the polyguanidine prepared are shown in Figure 1.

Most of the carbodiimides were prepared following literature methods. Monomers **III**, **IV**, and **V** and their

Scheme 1^a

^a (a) SOCl_2 , toluene; (b) azidotrimethylsilane, toluene; (c) *n*-hexyl (III, IV) or *n*-dodecylamine (V), CHCl_3 ; (d) corresponding phenol, KOH /ethanol; (e) PPh_3 , triethylamine, Br_2 , CH_2Cl_2 .

polymers were synthesized following the multistep route shown in Scheme 1. The polymerization of carbodiimides by the titanium half-metallocenes are living, reversible polymerizations with large, negative ΔS_{polym} values (e.g., -33 to -38 $\text{cal mol}^{-1} \text{K}^{-1}$) and comparatively small ΔH_{polym} (-13.5 to -14.1 kcal mol^{-1}). Hence, they have relatively low ceiling temperatures, T_c (e.g. I, 80 °C; *rac*-II, 153 °C; and *R*-II, 157 °C).³¹ Therefore, carbodiimide polymerizations should be carried out at room temperature and at the highest possible monomer concentrations. All polymerizations proceeded smoothly, and high yields were obtained in all cases. Liquid monomers I, *rac*-II, *R*-II, and V were polymerized in bulk, whereas the solid monomers with mesogenic side chains III, IV, and V were polymerized in concentrated chloroform solutions. The chemical structures of all the monomers and polymers were confirmed by ^1H NMR, ^{13}C NMR, IR spectroscopy, and elemental analysis. All of the resulting polymers except for poly-III showed high solubilities in common organic solvents and were therefore deemed suitable for this study.

Lytropic main-chain liquid crystallinity of poly-(*rac*-II) and poly-(*R*-II). From viscosity measurements it was determined that poly-(*rac*-II) displays lyotropic liquid crystalline phases above a critical concentration of about 20%. The optical polarizing microscopic image of poly-(*rac*-II) obtained from a 35% (w/w) solution in toluene is shown in Figure 2.

Poly-(*rac*-II) exhibited a threaded schlieren texture, indicating a nematic mesophase. The formation of the nematic mesophase was confirmed by X-ray diffraction studies (Figure 3).

In the X-ray diffractogram, a broad peak over a wide range of angles was observed, which is characteristic of a nematic mesophase. In contrast, another achiral polymer, poly-I, showed a lyotropic smectic mesophase under similar conditions.²⁵ The decrease in order between poly-I and poly-(*rac*-II) is attributed to the uniformity of the side chains (di-*n*-hexyl) in the former and the lack thereof in the latter (methyl and 2-phen-

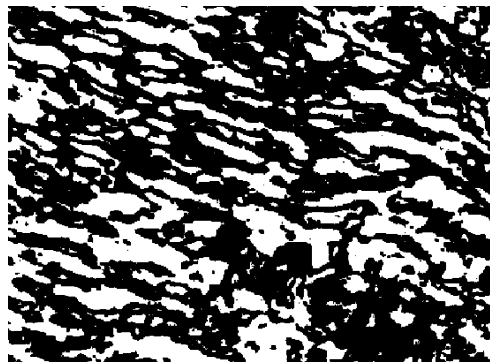


Figure 2. Optical polarizing microscopic image of a 35% (w/w) solution of poly-(*rac*-II) in toluene at room temperature ($500\times$).

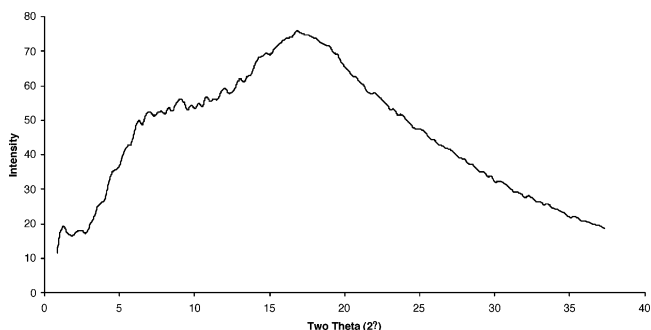


Figure 3. X-ray diffractogram of a 30% (w/w) solution of poly-(*rac*-II) in toluene at room temperature.

ylethyl). The uniform side chains of poly-I form a relatively impenetrable corona that holds adjacent polymer chains at a uniform distance apart. The dissimilar side chains of poly-(*rac*-II) are unable to provide the same effective barrier between backbones, and lateral disorder arises.

Fixing the chirality of the side chains has a profound effect on the properties of the polyguanidines, and this includes their liquid crystalline properties. Homochiral

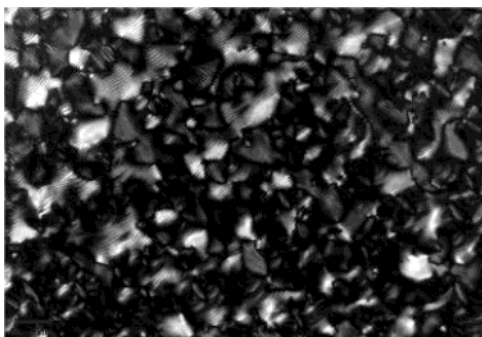


Figure 4. Optical polarizing microscopic image of the 12% solution (w/w) of poly-(*R-II*) in chloroform at room temperature (500 \times).

side chains impart a diastereometric relationship between the right- and left-handed helical conformations, and if the helix inversion barrier is low enough, then single-handed helices will be formed.^{32,33} The optical polarizing microscopic image of poly-(*R-II*) shown in Figure 4 was obtained from the 12.5% (w/w) solution in chloroform.

This chiral polymer showed a prototypical cholesteric mesophase, which results when the helical backbones adopt a single-handed screw sense.³⁴ It is well-known that liquid crystalline mesophase formation is dependent on the stiffness of the backbone. Compared to poly-(*rac-II*), poly-(*R-II*) forms mesophases at much lower concentrations at identical temperature. This implies that optically pure polymer is stiffer than the racemic polymer, and this is consistent with our light scattering and thermal analysis experiments.²⁶

Lytropic Liquid Crystallinity of the Combined-Type Polyguanidines, Poly-III and Poly-IV. One might think of the chiral helical backbone as a scaffold to build polymers with useful properties for use in fields such as nonlinear optics. This particular application would require appending polarizable mesogens as side chains. As these side chains could impart their own influence on the intermolecular alignment of these helices, we decided to explore the properties of polyguanidines with mesogenic side chains. The ease of preparation of carbodiimides with various side chains has allowed us to examine systems in which two distinct mesogens, showing different mesophase propensities, are combined within the same polymer. In this case, the stiff polyguanidine backbone with dissimilar size side chains and its preference for nematic phases was combined with small mesogens that favor smectic phase formations.

Three carbodiimide monomers having a mesogenic side chain were prepared following the synthetic route summarized in Scheme 1. Monomers **III**, **IV**, and **V** all have dissimilar side chains and would be expected to form polymers that adopt nematic phases. However, the biphenyl and diphenylazo mesogens of the sides should promote smectic ordering. These monomers were polymerized to form poly-**III** and poly-**IV**, respectively. The first isolated poly-**III** and poly-**IV** were found to be semicrystalline as shown in their X-ray diffractogram (Figure 5).

While poly-**III** shows one strong peak at $2\theta = 7.6^\circ$, which corresponds to a long-range spacing of 11.6 Å. Poly-**IV** shows a relatively small and broader peak at low angle ($2\theta = 7.7^\circ$), which corresponds to a long-range spacing of 11.5 Å. Additionally, poly-**III** shows stronger and sharper peaks at higher angle region, compared to

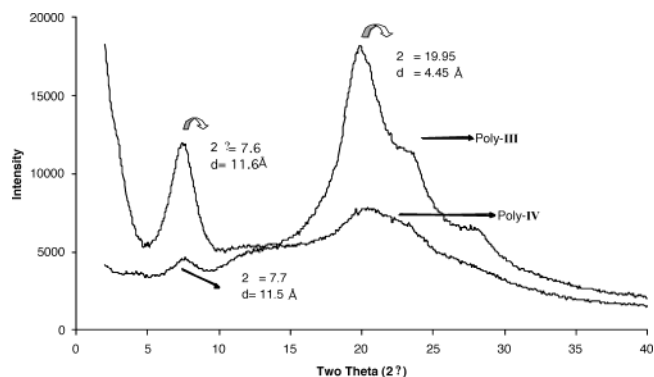


Figure 5. X-ray diffractograms of poly-**III** and poly-**IV** in solid state at room temperature.

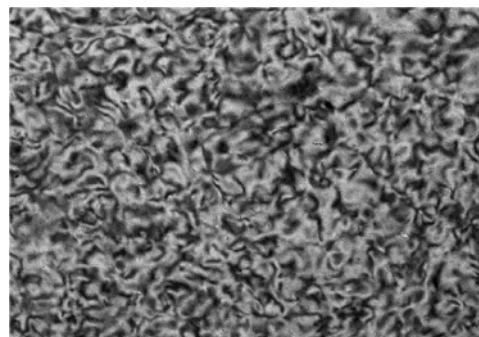


Figure 6. Optical polarizing microscopic image from a 21.4% (w/w) solution of poly-**IV** in 1,1,2,2-tetrachloroethane at 65 °C (200 \times).

poly-**IV**, indicating poly-**III** has more ordered structure of side chains than poly-**IV** in solid state. It should be noted that both of these polymers show smaller interchain spacing than that observed for poly-**I** with its two *n*-hexyl side chains. Even though half the side chains are longer in poly-**III** and poly-**IV**, the side-chain mesogens apparently accommodate a larger degree of interpenetration than the pure alkyl chains. Unfortunately, the lyotropic liquid crystalline properties of poly-**III** could not be investigated because concentrations exceeding the critical concentration of the polymer in solution could not be reached due to its poor solubility. The azo-mesogen appendage proved to be a better candidate, and the optical polarizing microscopic image of poly-**IV** is shown in Figure 6. From small-angle diffraction studies, it was determined that poly-**IV** forms a nematic mesophase. This, combined with the shorter interchain spacing suggests that the mesogenic side chains may pack parallel to the main-chain axis.

Poly-**V** with its longer C12 space and side chain proved to be sufficiently soluble to allow us to study the solution behavior of this derivative possessing the biphenyl mesogens. Like poly-**IV**, this derivative also displayed a lyotropic nematic mesophase. Its more interesting thermotropic behavior is discussed below. We conclude from this study, in which we compete mesogens with opposing propensities for phase behavior, the backbone appears to dominate (i.e., in this case at least, the tail does not wag the dog).

Thermotropic Liquid Crystalline Properties of Polyguanidines, Poly-V and Poly-VI. Polyguanidines have the unusual property of quantitatively depolymerizing back to monomer at relatively low temperatures (ca. 150–200 °C). Since nearly all of polyguanidines depolymerize before any melt transitions, thermotropic

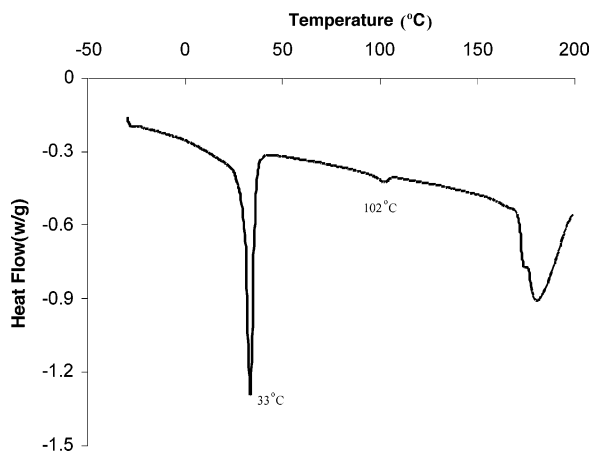


Figure 7. DSC thermogram of poly-VI.

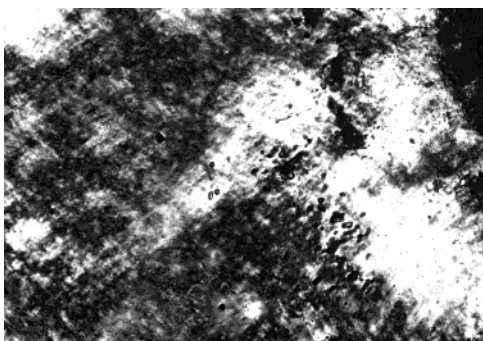


Figure 8. Optical polarizing microscopic image of poly-VI at 118 °C (200 \times).

liquid crystalline properties of these materials have never been observed. When we were preparing these polyguanidine derivatives with long side chains to increase the interchain spacing, we found that these polymers would display melt transitions. Interestingly, poly-VI shows two phase transitions in the DSC thermogram before its decomposition (Figure 7). The first transition at 33 °C is assigned to the melting of the C12 alkyl side chains. A second endothermic transition is observed at 102 °C and corresponds to a thermotropic mesophase formation—as evidenced by polarized optical microscopy (Figure 8)—that persists until the decomposition temperature of \sim 175 °C. X-ray diffraction studies were performed in the solid state at room temperature and at 118 °C. At room temperature, a strong sharp peak at low angle ($2\theta = 5.4^\circ$) corresponds to the long-range layer spacing, 16.4 Å, which is expectedly larger than the 13 Å spacing measured for the di-*n*-hexyl case of poly-I. Above the second endotherm at 118 °C, no large differences were observed except for a slight shift of the long-range spacing peak to lower angle, which is consistent with the extension of the alkyl side chains at such a high temperature. The mesophase behavior of this polymer can be described as helical rods ordered and aligned in molten paraffin.

Unlike poly-VI which possesses equivalent alkyl chains, poly-V, with its mixed C12 and C12 mesogenic side chains, shows no side-chain melting in the DSC trace. It thus appears that the terminal biphenyl mesogen prevents alkyl side chain crystallization in this derivative, but it does induce an order of its own (vide infra). Poly-V does show a reversible phase transition at 119 °C, and the cross-polarized micrograph provides evidence of mesophase formation above this temperature (Figure 9).

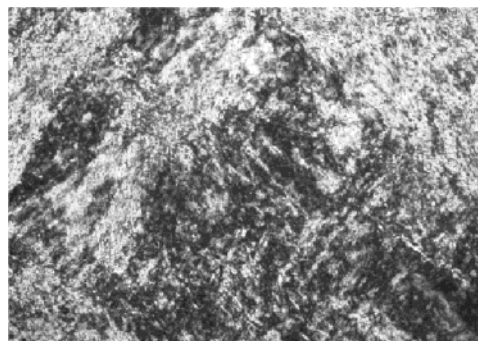


Figure 9. Optical polarizing microscopic image of poly-V at 130 °C (200 \times).

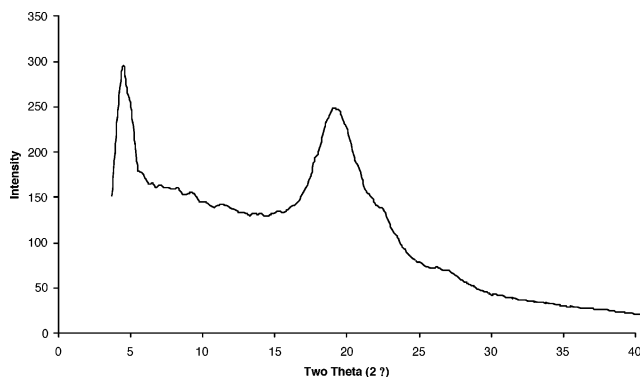


Figure 10. X-ray diffraction pattern of poly-V at 130 °C.

The X-ray diffraction patterns were measured at room temperature and 130 °C. At 130 °C, the X-ray pattern of poly-V appears the same as that at room temperature, with both showing low-angle peaks at approximately $2\theta = 5^\circ$. This provides evidence for a smectic layered structure with spacing 18–20 Å that is maintained in the high-temperature mesophase (Figure 10). At high angle, the peaks are sharper than seen in poly-VI, which implies an ordered side chain structure between the main chains at both room temperature and 130 °C. Unlike in solution, where nematic phases preferred by the stiff backbone are favored, the thermotropic mesophases appear to be influenced by the side-chain mesogens, and smectic layered structures result. In this case, the tail does appear to wag the dog.

Conclusion

With the goal of establishing some of the rules governing the liquid crystallinity of the helical polyguanidines, we prepared several derivatives and investigated their lyotropic—and in some cases thermotropic—properties using optical polarizing microscopy and X-ray diffraction. Each repeat unit of these polymers possesses two side chains, and if these are identical, the polymer can adopt a more ordered, layered structure in both solution and the solid state. Examples include poly-I and poly-VI, which possess di-*n*-hexyl and di-*n*-dodecyl side chains, respectively. This higher level of ordering is believed to arise from the formation of a dense corona barrier that effectively acts to uniformly separate the helical backbones. When the side chains differ in length, e.g., poly-(*rac*-II) and poly-IV, the uniform layering breaks down and a simpler nematic structure arises. Chirality also plays a very important role. Fixed, homochiral side chains, e.g., poly-(*R*-II), force all of the chains to adopt a preferred helical sense, and these screws now pack in a cholesteric mesophase. Further-

more, poly-(**R-II**) displays mesophases at lower concentrations than poly-(**rac-II**) (12% vs 20%, respectively), implying that poly-(**R-II**) is stiffer than its racemic counterpart.

We also explored combined systems in which the liquid crystalline backbones were elaborated with side-chain mesogens to ask the question of which mesogenic moiety will dominate the observed behavior. In solution, the backbones of poly-**IV** and poly-**V** appeared to dominate, and nematic phases were observed. In the melt, however, a layered smectic phase was observed for poly-**V**, and this is attributed to the influence of the side-chain mesogens. Interestingly, poly-**V**, similar to poly-**IV**, exhibited thermotropic liquid crystalline behavior between 102 °C and the decomposition temperature of ~175 °C. Both poly-**V** and poly-**VI** displayed thermotropic smectic mesophases, and poly-**V** with its mesogenic side chains showed more ordered alignment of side chains at 130 °C. These are the first thermotropic mesophases observed for any of the polyguanidines prepared to date.

Acknowledgment. The authors acknowledge the NSF for financial support of this work.

References and Notes

- Panar, M.; Phillips, W. D. *J. Am. Chem. Soc.* **1968**, *90*, 3880.
- Robinson, C. *Trans. Faraday Soc.* **1956**, *52*, 571. (b) Robinson, C.; Ward, J. C.; Beevers, R. B. *Discuss. Faraday Soc.* **1958**, *25*, 29. (c) Troxell, T. C.; Scheraga, H. A. *Macromolecules* **1971**, *4*, 528.
- Elliot, A.; Ambrose, E. J. *Discuss. Faraday Soc.* **1950**, *9*, 246.
- Samulski, E. T. *Liquid Crystalline order in Polymers*; Academic Press: New York, 1978; p 167.
- Dupre, D. B. *Polym. Eng. Sci.* **1981**, *21*, 717.
- Dupre, D. B. *J. Appl. Polym. Sci., Appl. Polym. Symp.* **1985**, *41*, 69.
- Jeremic, K.; Karasz, F. E. *Eur. Polym. J.* **1983**, *19*, 1037.
- Sakamoto, R. *Colloid Polym. Sci.* **1984**, *262*, 788.
- Miller, W. G.; Russo, P. S.; Chakrabart, S. *J. Appl. Polym. Sci., Appl. Polym. Symp.* **1985**, *41*, 49.
- Miller, W. G. *Annu. Rev. Phys. Chem.* **1978**, *29*, 519.
- Nolte, R. J. M.; Drenth, W. *Pays-Bas* **1973**, *92*, 788.
- Millich, F.; Hellmuth, E. W.; Huang, S. Y. *J. Polym. Sci., Polym. Chem. Ed.* **1975**, *13*, 2143.
- Millich, F. *Adv. Polym. Sci.* **1975**, *19*, 117.
- Millich, F. *Macromol. Rev.* **1980**, *15*, 207.
- Aharoni, S. M. *J. Polym. Sci., Polym. Phys. Ed.* **1979**, *17*, 683.
- Aharoni, S. M. *J. Macromol. Sci., Phys.* **1982**, *21*, 105.
- Aharoni, S. M. *Macromolecules* **1979**, *12*, 94.
- Bur, A. J.; Fetters, L. J. *Macromolecules* **1973**, *6*, 874.
- Bur, A. J.; Roberts, D. E. *J. Chem. Phys.* **1969**, *51*, 406.
- Aharoni, S. M. *Macromolecules* **1981**, *14*, 222.
- Aharoni, S. M.; Walsh, E. K. *Macromolecules* **1979**, *12*, 271.
- Aharoni, S. M. *J. Polym. Sci., Polym. Phys. Ed.* **1980**, *18*, 1439.
- Goodwin, A.; Novak, B. M. *Macromolecules* **1994**, *27*, 5520.
- Nieh, M.; Goodwin, A.; Stewart, J.; Novak, B. M.; Hoagland, D. A. *Macromolecules* **1998**, *31*, 3151.
- Kim, J.; Novak, B. M.; Waddon, A. J. *Macromolecules* **2004**, *37*, 1660.
- In contrast, the related polymer, poly(*N*-hexylisocyanate), with its lower density of side chains forms only nematic lyotropic phases. See refs 15–22.
- Shibayama, K.; Seidel, S. W.; Novak, B. M. *Macromolecules* **1997**, *30*, 3159.
- Pawlowski, N. E.; Lee, D. J.; Sinnhuber, R. O. *J. Org. Chem.* **1972**, *37*, 3245.
- Kawakami, Y.; Toida, K. *Macromolecules* **1995**, *28*, 816.
- Burmistrov, V. A.; Kuzmina, S. A.; Koifman, O. I. *Russ. J. Org. Chem.* **1995**, *31*, 351.
- Goodwin, A. A. PhD thesis. The Synthesis and Characterization of Polycarbodiimides, University of California, Berkeley, 1996.
- Schlitzer, D. S.; Novak, B. M. *J. Am. Chem. Soc.* **1998**, *120*, 2196.
- Tang, H.-Z.; Tian, G.; Capracotta, M. D.; Novak, B. M. *J. Am. Chem. Soc.* **2004**, *126*, 3722.
- Tian, G.; Lu, Y.; Novak, B. M. *J. Am. Chem. Soc.* **2004**, *126*, 4082.

MA0493527